

Solid tumor risks after high doses of ionizing radiation

Rainer K. Sachs*[†] and David J. Brenner*^{‡§}

Departments of *Mathematics and [†]Physics, University of California, Berkeley, CA 94720; and [‡]Center for Radiological Research, Columbia University, 630 West 168th Street, New York, NY 10032

Communicated by Richard Doll[¶], Cancer Research UK, Oxford, United Kingdom, August 3, 2005 (received for review March 25, 2005)

There is increasing concern regarding radiation-related second-cancer risks in long-term radiotherapy survivors and a corresponding need to be able to predict cancer risks at high radiation doses. Although cancer risks at moderately low radiation doses are reasonably understood from atomic bomb survivor studies, there is much more uncertainty at the high doses used in radiotherapy. It has generally been assumed that cancer induction decreases rapidly at high doses due to cell killing. However, recent studies of radiation-induced second cancers in the lung and breast, covering a very wide range of doses, contradict this assumption. A likely resolution of this disagreement comes from considering cellular repopulation during and after radiation exposure. Such repopulation tends to counteract cell killing and accounts for the large discrepancies between the current standard model for cancer induction at high doses and recent second-cancer data. We describe and apply a biologically based minimally parameterized model of dose-dependent cancer risks, incorporating carcinogenic effects, cell killing, and, additionally, proliferation/repopulation effects. Including stem-cell repopulation leads to risk estimates consistent with high-dose second-cancer data. A simplified version of the model provides a practical and parameter-free approach to predicting high-dose cancer risks, based only on data for atomic bomb survivors (who were exposed to lower total doses) and the demographic variables of the population of interest. Incorporating repopulation effects provides both a mechanistic understanding of cancer risks at high doses and a practical methodology for predicting cancer risks in organs exposed to high radiation doses, such as during radiotherapy.

second cancer risks | radiotherapy

There is increasing concern regarding radiation-related second-cancer risks in long-term radiotherapy survivors (1, 2) and a corresponding need to be able to understand and predict cancer risks at high radiation doses (3). Cancer risks after acute exposure to ionizing radiation at intermediate doses, up to approximately 3 Gy, are reasonably well understood, based mainly on data from atomic bomb (A-bomb) survivors; however, there is considerably more uncertainty about the effects of higher doses (3). Because of the high doses inevitably given to organs close to a tumor during radiotherapy, the issue of radiation-induced second cancers at high doses is increasingly important (1), particularly in light of the large number of cancer patients undergoing high-dose (65–80 Gy) radiotherapy, at younger ages (4), and with increasing survival times (5).

It has usually been assumed that cancer induction decreases rapidly at higher doses due to cell killing, in that dead cells cannot give rise to a malignancy, and cell survival decreases exponentially or even faster with increasing dose (6, 7). A standard quantitative implementation of this “initiation + killing” mechanism, in which the high dose risks are dominated solely by a balance between carcinogenic alteration and cell killing, is reproduced in most radiation biology text books (8, 9) (see also curves in Fig. 1 and *Supporting Text*, which is published as supporting information on the PNAS web site). This standard

high-dose model has frequently been used to analyze data on radiation-induced carcinogenesis (7, 10–15).

Until recently, almost all studies on second-cancer risks at high doses [comprehensively surveyed in 2001 by Little (14)] have been restricted to single data points in each study, and considerable interstudy variability made the assessment of dose-risk trends very uncertain. However, several studies of radiation-induced second cancers in Hodgkin’s disease patients have recently been published (16–18), which cover a very wide range of radiation doses, and now provide intrastudy stratifications of cancer risk as a function of dose to the tumor location.

These more recent epidemiological data on second cancer risks stratified by dose (16–18) are shown in Fig. 1. Also shown are the corresponding cancer incidence data from A-bomb survivors (19, 20), indicating the lower-dose region for which the cancer risks are comparatively well known. The curves in Fig. 1 show the predictions of the standard “initiation + killing” model, discussed above, fitted to these A-bomb cancer-incidence data. Even considering the uncertainties of the parameters estimated in the fit to the A-bomb data (15) and their transfer to a Western population (21), as well as corrections for dose fractionation (see *Supporting Text*), it is clear that the standard “initiation + killing” model of cancer risks results in predictions of cancer risks at high doses that are entirely inconsistent with the newer epidemiological data, neither the measured breast-cancer nor lung-cancer risks decrease with increasing dose over the approximate dose range from 3 to 40 Gy.

A likely resolution of this disagreement comes from the fact that repopulation of normal tissue is known to occur during and after fractionated high-dose exposure (22–27). Such repopulation tends to counteract cell killing (28–33) and thus might account for the major discrepancies between the standard model and the recent data illustrated in Fig. 1. We therefore describe here a systematic, biologically based, quantitative model for the dose dependence of radiation-induced cancer risks at high doses, emphasizing fractionated exposures, such as are used in radiotherapy. The model incorporates carcinogenic effects, cell killing, and additionally cell proliferation/repopulation effects, using a minimum of adjustable parameters. We use this model to analyze and predict dose–response data for second solid cancer induction, at fractionated high radiation doses.

Methods

Our goal is to predict the shape of the dose–response relations for organ-specific radiation-induced solid cancer risks in any given demographic population, from intermediate to very high doses. As in the standard model (6, 7), this shape will be based on the predicted yield, M , of premalignant stem cells associated with the radiation exposure to a given organ at a given dose. The

Freely available online through the PNAS open access option.

Abbreviations: ERR, excessive relative risk; A-bomb, atomic bomb.

[§]To whom correspondence should be addressed. E-mail: djb3@columbia.edu.

[¶]Deceased July 24, 2005.

© 2005 by The National Academy of Sciences of the USA

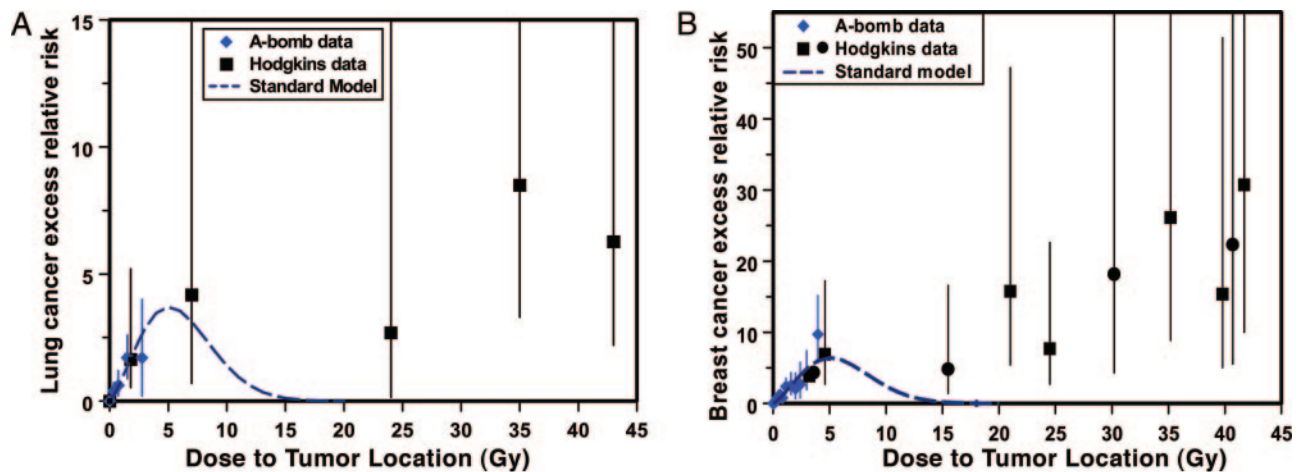


Fig. 1. Excess relative risks for radiation-induced lung cancer (*A*) and female breast cancer (*B*). The data points from A-bomb survivors (19, 20) are at moderate doses (<4 Gy). The data points at high doses are from studies of second cancers after radiotherapy of Hodgkin's disease patients: lung cancer, median age at exposure 45, median age at second cancer 58 (18); and breast cancer, median age at exposure 23, median age at second cancer 42 (16, 17). In the published reports, the breast cancer risks for Hodgkin's disease patients were internally normalized to the lowest-dose group [mean dose 3.2 Gy for Travis *et al.* (16) and 3.6 Gy for van Leeuwen *et al.* (17)]; these breast cancer data (*B*) have here been renormalized based on the estimated A-bomb excess relative risks for breast cancer (19) at 3.2 and 3.6 Gy, respectively, adjusted for the different demographics and background risks of the Hodgkin's breast cancer patients vs. the A-bomb survivors. The data points for lung cancer (*B*) are taken directly from the published data (18). The dashed curves represent fits to the A-bomb data using the standard "initiation + killing" model (refs. 6 and 7 and see *Supporting Text*), which involves a balance solely between induction of premalignant cells and cell killing, without considering cellular repopulation. As discussed in the text, it is clear that the predictions of this standard model are inconsistent with the high-dose data.

radiation-associated risk will be taken as proportional to this yield, the assumption being that subsequent long-term evolution of a cancer from premalignant cell(s) will not markedly change the shape of the dose-response relation, although the magnitude of the long-term cancer risk will, of course, depend also on the demographic variables of the population of interest.

We thus describe a model that tracks the fate of an organ's stem cells (34), pluripotent cells capable of regenerating normal tissue (35, 36) but that are also the primary cells at risk for a radiation-induced event that can eventually lead to cancer (37). We assume that (i) radiation increases the number of stem cells in the organ that undergo a rate-limiting step on the path to carcinogenesis (i.e., become "pre-malignant"); (ii) radiation-induced cell killing has a standard, well understood dose dependence (38, 39); and (iii) during and shortly after radiotherapy, the organ's stem cells respond to radiation-induced cell-killing exposure through accelerated repopulation, which, under feedback control, tends to homeostatically restore their number back to their original steady-state or setpoint number N (26, 27). As discussed above, this approach emphasizes biological processes during the period, lasting a number of weeks, from the start of radiation exposure until the relevant organ has repopulated. Subsequent carcinogenesis steps occurring on a substantially longer time scale are not analyzed explicitly, in that they are not expected to change the shape of the dose-risk relations but are implicitly considered in the appropriate proportionality factor, discussed below, relating the yield of premalignant cells to the excess relative risk for the population of interest.

Estimation of the Yield of Premalignant Stem Cells. Our initial goal is to estimate the yield, M , of radiation-associated premalignant cells present in the organ at the time when repopulation has finished, i.e., when the number of stem cells in the organ has returned to its original steady-state number, N .

Consider a fractionated radiation exposure protocol with K separate dose fractions, where the dose per fraction at a given location in an organ is d . Suppose, for simplicity, that the time between fractions is a fixed interval T . We track the time evolution of the expected numbers of normal (n) and of radia-

tion-mutated premalignant (m) stem cells. Here n and m are, respectively, mnemonics for normal and premalignant cell growth pathways. In all our analyses, $m \ll n$. Let $n^-(k)$ denote the expected number of normal stem cells just before the k th dose fraction, with $k = 1, 2, \dots, K$; let $n^+(k)$ denote the expected number just after the k th fraction and, similarly for premalignant stem cell numbers, $m^-(k)$ and $m^+(k)$. The following equations track the time evolution of m and n :

$$n^+(k) = S P n^-(k), \quad [1]$$

where

$$S = \exp(-\alpha d) \text{ and } P = \exp(-\gamma d) \approx 1 - \gamma d;$$

$$m^+(k) = S[m^-(k) + (1 - P)n^-(k)]; \quad [2]$$

$$n^-(k+1) = N / \{1 - e^{-\lambda T} [1 - N/n^+(k)]\}; \quad [3]$$

$$m^-(k+1) = m^+(k) [n^-(k+1)/n^+(k)]^r. \quad [4]$$

Eqs. 1 and 2 describe the effect of a single dose fraction, in a manner similar to that described by Wheldon and coworkers (30, 33). In Eq. 1, the parameter α is the number of normal stem cells killed per unit dose per surviving normal stem cell, and thus S is the surviving cell fraction after one dose fraction, d . γ is interpreted as the number of premalignant stem cells produced per unit dose per normal stem cell, and so P is the fraction of normal stem cells that are not made premalignant in one dose fraction. Eq. 2 thus describes the situation where the number of premalignant cells just after a dose fraction is the number that survive from just before the fraction, plus the number of cells that are made premalignant by, and survive, that dose fraction.

Eqs. 3 and 4 implement our approach of incorporating radiation-induced accelerated repopulation/proliferation of normal and premalignant stem cells, both between dose fractions and after the last dose fraction. Eq. 3, involving a positive repopulation rate constant λ , describes a homeostatic tendency for the number of normal stem cells in a given organ, n , to increase whenever it falls below the original steady-state setpoint number (N) of stem cells in the organ. As discussed more fully in

Supporting Text, Eq. 3 is based on a standard logistic equation (27, 40), so that the smaller the number of surviving normal stem cells, the larger the per-cell repopulation rate.

Finally, Eq. 4 describes proliferation for the premalignant cells. It is possible that the growth kinetics of the premalignant cells will differ from that of the normal cells, due for example to changes in reproductive death or apoptosis (41–43). We assume that the repopulation kinetics of the premalignant cells will follow the same basic pattern as those of the normal stem cells, but with the possibility that the per-cell growth rate of premalignant cells differs by a constant factor r from the per-cell growth rate for normal stem cells. As shown in Supporting Text, this scenario leads to Eq. 4.

Eqs. 1–4 can be simplified or generalized. Details of a useful and apparently realistic simplification are given in Results. The equations can be generalized by allowing: linear-quadratic instead of linear expressions for log-killing and/or induction of premalignant cells (Eq. 1), different times between different fractions (Eq. 3, e.g., no treatments on weekends), different doses for different fractions, a time lag before accelerated repopulation sets in, and different repopulation models (30); by including the effects of cell killing and repopulation on premalignant cells already present before the start of radiotherapy; and/or by using Markov chain generalizations of Eqs. 2 and 4 to take into account stochastic fluctuations in the number of premalignant cells. Details are given in Supporting Text. Incorporating any or all of these generalizations leads only to quite minor changes in the basic arguments, calculations, results, and conclusions presented here.

Eqs. 1–4 can be solved numerically by using an iterative technique, starting from the appropriate initial conditions just before the first fraction, namely $n^-(1) = N$ and $m^-(1) = 0$ (Fig. 2). The iterative procedure yields the stem cell numbers just after the last fraction, namely $n^+(K)$ and $m^+(K)$. If $k = K$ in Eqs. 3 and 4, these equations give $n(T)$ and $m(T)$ at any time interval T after the last fraction. The number of radiation-associated premalignant cells, M , present at the subsequent time when the number of normal stem cells has returned to its original steady-state number, N (and thus repopulation effectively ceases, see Fig. 2), is given by Eq. 4 as:

$$M = m^+(K)[N/n^+(K)]^r. \quad [5]$$

In the application of Eqs. 1–4 to the data (16–18) considered in the present paper, the total dose D to the location of the second cancer ranged from 3 to 45 Gy, with the dose d per fraction taken as $D/20$ (20 being the typical number of dose fractions used).

Numerical solutions, validated analytically by applying linear perturbation theory to Eqs. 1–5, show that for a sufficiently small total dose D , e.g., $D \leq 5$ Gy, the number M of radiation-associated premalignant stem cells present after repopulation has ceased is essentially linear in dose. Specifically,

$$M = \gamma ND, \quad [6]$$

at sufficiently low doses, a result consistent with the approximate linear dose dependencies of individual solid cancer risks in A-bomb survivors (20, 44).

Solid Cancer Risk Estimates at High Doses, Based on the Yield of Premalignant Stem Cells. The dose- and organ-specific excess relative risk (ERR) is estimated by using Eqs. 1–5 to estimate M , the yield of radiation-associated premalignant stem cells present in the organ when repopulation has ceased (Fig. 2). This estimate of M is used together with our proportionality assumption for risks in the form

$$ERR = M \times B. \quad [7]$$

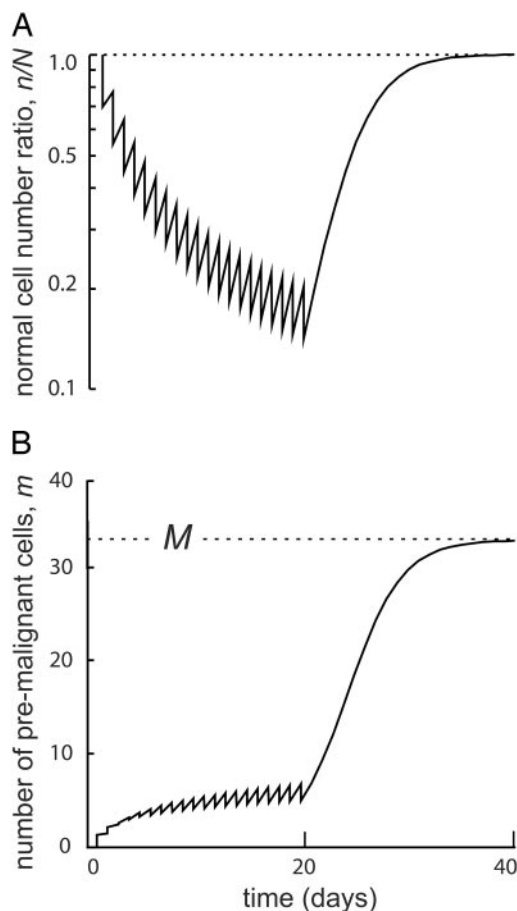


Fig. 2. Normal and premalignant stem cell numbers as a function of time during and after irradiation. (A) The predictions of Eqs. 1 and 3 for the number, n , of normal stem cells as a function of time for 20 daily fractions of $d = 2$ Gy each, with cell killing parameter $\alpha = 0.18$ per Gy and repopulation rate $\lambda = 0.4$ per day. Initially, n has its setpoint value N , so the ratio shown is 1. At each fraction, n is decreased by killing, then some repopulation occurs between fractions. The repopulation is accelerated; in this logarithmic plot, the acceleration is manifested by the fact that the vertical height of the repopulation is larger between later fractions than near the start of irradiation. After irradiation stops, n gradually returns to its set point value N , here effectively reaching N at about day 40. Similar patterns hold if there is no treatment on weekends (see Supporting Text). (B) The number, m , of radiogenic premalignant cells (Eqs. 2 and 4). Parameters are those used for n in A and the following: setpoint $N = 10^6$, initiation parameter $\gamma = 10^{-6}$ per Gy, and repopulation ratio $r = 0.96$. Each fraction produces some new premalignant cells as well as killing some premalignant cells already present. Between fractions, there is repopulation of premalignant cells, essentially tracking the repopulation of normal stem cells (Eq. 4). After irradiation stops, m continues to track n until at 40 days it has almost reached a plateau value M (Eq. 5). The models of this paper do not explicitly consider cell proliferation patterns for longer time scales, which may differ, both for normal and for premalignant cells.

M depends on the dose and fractionation protocol, as well as, in general, on parameters describing induction, killing, and repopulation (see Eqs. 1–4). B is a proportionality factor linking the yield of premalignant cells to the risk. B is independent of radiation parameters but will generally depend on demographic and cohort factors such as nationality, sex, age at exposure, attained age, latency period, smoking patterns, etc. Describing ERR as the product of a dose-dependent term (M) and a proportionality term (B) describing modifying factors is a standard approach (18, 21).

The proportionality term, B , is estimated for the tumor site and demographic population of interest by noting that it is

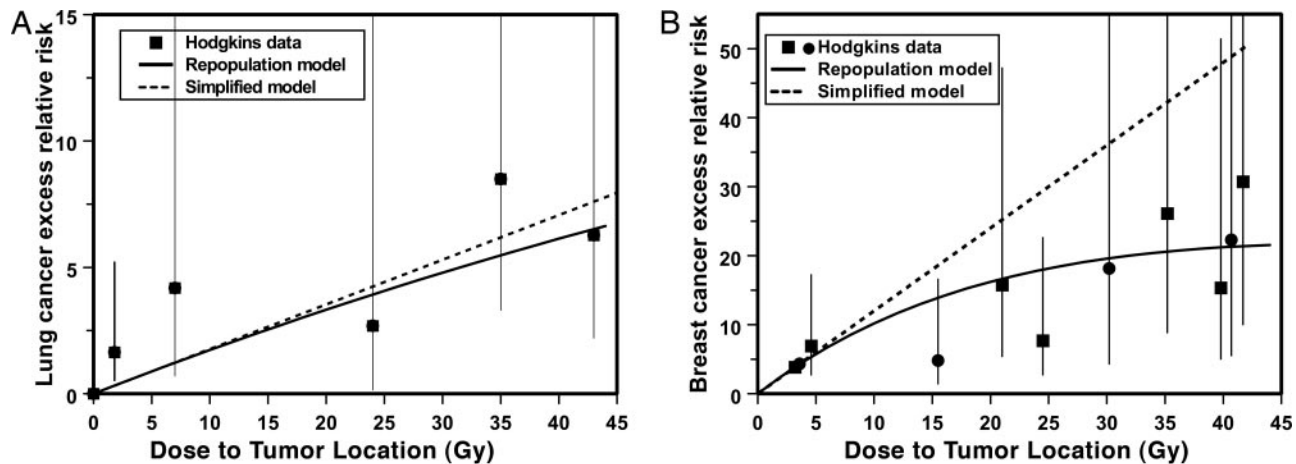


Fig. 3. Measured and predicted excess relative risks for lung cancer (A) and female breast cancer (B) induced by high doses of ionizing radiation. The data points are from studies of second cancers after radiotherapy of Hodgkin’s disease patients (16–18), as in Fig. 1. The dashed lines are the predictions of the simplified repopulation model (Eq. 13), which has no free parameters: its single relevant parameter, the slope at low doses, is derived from the excess relative risks of the A-bomb survivors for lung and breast, respectively, adjusted for the different demographic variables of the Hodgkin’s patients vs. the A-bomb survivors [after adjustment $(ERR/D)_{lung} = 0.18/Gy$, $(ERR/D)_{breast} = 1.2/Gy$]. In B, that the points near 3.5 Gy (shown without error bars) fall exactly on the dashed line is automatic, given our renormalization procedure described in Fig. 1, but the approximate fit for the other points is an intrinsic property of the data. The solid curves are the predictions of the repopulation model (Eqs. 1–4), which allows different repopulation rates for normal vs. premalignant stem cells. For these curves, the initial slope was fixed as above; the cell killing parameter α (see Eq. 1) was fixed at 0.18/Gy (39). The other two free parameters, obtained by adjusting to the data shown, are the ratio of the per cell growth rates, r (see Eq. 4, $r_{lung} = 0.96$, $r_{breast} = 0.76$), and the repopulation rate parameter λT (see Eq. 3, $\lambda T = 0.4$ for both lung and breast).

proportional to the slope at low doses of the excess relative risk, ERR/D . Specifically, from Eqs. 6 and 7,

$$ERR/D = \gamma NB, \quad [8]$$

at doses pertinent to the A-bomb survivor data.

We then take advantage of the formalism described, for example, by Land *et al.* (21), to estimate the site-specific ERR/D for A-bomb survivors and then to adjust this value to apply to different cohorts with different demographic properties. The result is the low-dose slope, and thus the parameter γNB , for the site and demographic population of interest.

Results

We implemented the transfer of risks from A-bomb survivors by using Eq. 8 and publicly available software (21), thereby determining initial slopes, γNB , of the ERR dose–response curves for second cancers in the Hodgkin’s disease radiotherapy patients (Fig. 3); some details of the implementation are outlined in *Supporting Text*.

Once the initial slope, γNB , is fixed for a given site and demographic cohort, the only remaining parameter combinations relevant to the solutions of Eqs. 1–5 are the cell-killing parameter α , a repopulation rate factor λT , and the relative repopulation rate for premalignant vs. normal cells r ; for example, changing the parameter γ does not perceptibly change the solution, M , provided the initial slope, γNB , is held constant by a corresponding change in N . Dose–response relations for killing of human cells are comparatively well established, so that α can be treated as known within fairly narrow limits (38). This leaves two extra parameters that are needed to determine the high-dose cancer risk, λT and r . For the analysis described here, these two constants were established based on the high-dose second-cancer incidence data in Hodgkin’s disease patients (Fig. 1).

Results are shown in Fig. 3. It is seen that the model can provide a good description of the high-dose second-cancer risks. The data suggest a modest reduction in the repopulation rate of premalignant stem cells relative to normal stem cells during the

repopulation period for breast cells (ratio, $r = 0.76$) and a still more modest reduction (ratio, $r = 0.96$) for the lung.

Simplified Model. The best estimates for the repopulation ratio, r , were close to unity (0.96 for lung, 0.76 for breast). We therefore investigated the case $r = 1$, where damaged and undamaged stem cells repopulate at the same per-cell rate. In this situation, a major simplification occurs: the final cancer risks no longer depend perceptibly either on the killing parameter α or the repopulation parameter λT .

The underlying reason for this surprising simplification can be seen by writing more general equations for the time course of the normal and premalignant stem cell numbers:

$$dn/dt = Fn - \gamma Rn, \quad [9]$$

$$dm/dt = Fm + \gamma Rn, \quad [10]$$

where $R = R(t)$ is any dose-rate function, and F is any function of m , n , and R . The function F represents per-cell killing and repopulation, constrained to be the same in both equations by our assumption that premalignant and normal stem cells have identical killing and repopulation kinetics (corresponding to $r = 1$). As above, the function F is assumed to have a form that ensures that, after the irradiation stops, the number of normal stem cells, n , grows back to the organ’s steady-state setpoint number, N . The final term in both equations represents cells made premalignant by the radiation exposure.

Dividing Eq. 9 by n and Eq. 10 by m and subtracting gives a result in which the killing/repopulation function F has cancelled out (no matter what its functional form), as follows:

$$d[\ln(1 + m/n)]/dt = \gamma R. \quad [11]$$

For any dose fractionation scheme, i.e., for any dose rate function $R(t)$, Eq. 11 can be integrated to obtain, for all times after the end of the radiation exposure:

$$m = n[\exp(\gamma D) - 1]. \quad [12]$$

This remarkable result implies that when the number of stem cells in an organ grows back to the original steady-state setpoint number, N , then the corresponding number, M , of premalignant cells does not depend on the details of cell killing or of cell repopulation or the fractionation/protraction scheme of how the dose D is delivered. Specifically, the predicted excess relative risk is the same as if neither killing nor repopulation had occurred. Intuitively, what is happening is that cell killing decreases the number of normal cells at risk, and in addition some premalignant cells are killed by radiation, both effects tending to decrease risk; however, repopulation of normal and premalignant stem cells during and after treatment exactly compensates for these effects in terms of the number, M , of radiation-associated premalignant cells and thus the later cancer risk.

At all relevant doses (even those substantially above 5 Gy) $\gamma D \ll 1$ in Eq. 12, corresponding to $m \ll n$. This implies that, in the simplified model, the *ERR* is expected to be almost linearly related to the dose at all relevant doses (Fig. 3):

$$ERR = MB = N[\exp(\gamma D) - 1]B \approx \gamma NBD. \quad [13]$$

Eq. 12 and the approximation $\exp(\gamma D) - 1 \approx \gamma D$, used in Eq. 13, were validated through numerical computations; these confirmed that, for $r = 1$, when the number of stem cells in an organ grows back to the original steady-state setpoint number, the corresponding number, M , of premalignant stem cells does not depend on the details of cell killing or cell repopulation or on the dose fractionation/protraction scheme. As detailed in *Supporting Text*, setting $r = 1$ renders the values of all other parameters except the initial slope irrelevant, even when using linear-quadratic rather than just linear expressions for log survival, when using alternate repopulation models, or when analyzing premalignant cell numbers stochastically.

Because Eq. 13 applies to any fractionation/protraction dose scheme, it can be applied to the high-dose fractionated radiotherapy of the Hodgkin's disease patients (see Figs. 1–2). Specifically, we used Eq. 13 to predict the high-dose second-cancer incidence for breast and lung, based solely on cancer-incidence data for A-bomb survivors (19, 20). As before, the approach was to use estimates of the initial slope of the dose response, obtained from A-bomb cancer incidence data, adjusted for the different demographic and cohort properties of the Hodgkin's disease patients.

It can be seen from Fig. 3 that the simplified model, Eq. 13, produces predictions not inconsistent with the high-dose cancer risk data. The simplified prediction has the same initial slope as that for the more general model given by Eqs. 1–4 but no longer curves perceptibly at high doses. For the lung, the simplified $r = 1$ model is quite consistent with the high-dose data; for the breast, the simplified $r = 1$ model may overpredict the high-dose cancer risks by a factor of approximately 2–3. Because no free parameters at all are involved, the high-dose cancer risk predictions being entirely determined by A-bomb risk estimates modified by the appropriate cohort factors, even an overprediction by a factor of 2–3 is a very substantial improvement over current models (6), which predict essentially zero excess risk at doses above approximately 25 Gy (see Fig. 1 and *Supporting Text*).

Discussion

High-dose radiotherapy is being used with great success on a large number of cancer patients who may well live for many years

post radiotherapy. The 10-year relative survival rates for prostate cancer and breast cancer in the U.S. are now approximately 76% (45), so there is increasing concern about the possibility of second cancers in long-term radiotherapy survivors (1, 3). Epidemiological studies of second cancers are, by their nature, limited to radiotherapy techniques that were common several decades ago (1, 2). Thus it is important to be able to predict the carcinogenic effects of fractionated high doses of ionizing radiation, particularly on an organ-by-organ basis.

Both recent (16–18) and older (14) second-cancer data make it clear that solid cancer risks do not decrease rapidly at high doses, contrary to the predictions of the current standard model of high-dose cancer induction, which describes a balance solely between carcinogenic alteration and cell killing. On a mechanistic level, the analysis here indicates that significant levels of radiation-induced stem-cell repopulation counteract comparably large levels of radiation-induced cell killing, so that the overall response remains either linear or near linear.

Including the effect of radiation-induced stem-cell repopulation yields models (i) whose predictions are consistent with high-dose experimental data, and (ii) which provide a simple and practical approach to predict high-dose cancer risk for any type of radiotherapy exposure (fractionated, continuous, or acute), based only on cancer risk data from A-bomb survivors (who were exposed to lower doses), and the demographic variables of the target population of interest.

The simplified model described here requires no parameters except those determined by the A-bomb survivor data for any/all of the 21 solid organs for which risk estimates are available from the A-bomb survivors (20, 46). Based on the analyses here for breast and lung, even this simplified model should produce risk estimates at high doses good at least to within factors of 2 or 3, an enormous improvement on the standard “initiation + killing” model, which neglects repopulation.

The more general model given by Eqs. 1–4 can provide a rather better description of the high-dose data (Fig. 3), at the cost of using two extra, organ-dependent adjustable parameters describing radiation-induced accelerated repopulation. To use this more general model predictively, these two organ-dependent parameters need to be estimated from high-dose data, for example from recent studies of second cancers after radiotherapy for testicular cancer, which provide usable data at two high-dose points for stomach, small intestine, rectum, liver, gallbladder, pancreas, kidney, and bladder (47).

Additional generalizations of Eqs. 1–4, described in *Supporting Text*, involve additional adjustable parameters and appear to yield only marginal improvements.

As an example of the importance of understanding the shape of the dose–response relation at high doses, a model such as the current standard model shown in Fig. 1 would imply that organs very close to the tumor, which typically receive doses above 20 Gy, would be at very low risk for radiation-induced second cancers. By contrast, the data and the models discussed here would suggest that organs closest to the tumor, which received the highest doses, would be at the highest risk, which is clinically observed to be the case (2). These new models should also facilitate estimates of second-cancer risks after new types of high-dose radiotherapy, such as intensity-modulated radiotherapy (3, 48).

We thank Charles Land, Mark Little, Ethel Gilbert, Elaine Ron, and Eric Hall for helpful discussions.

- van Leeuwen, F. E. & Travis, L. B. (2004) in *Cancer: Principles and Practice of Oncology*, eds. Devita, V. T., Hellman, S. & Rosenberg, S. A. (Lippincott, Williams & Wilkins, Philadelphia).
- Brenner, D. J., Curtis, R. E., Hall, E. J. & Ron, E. (2000) *Cancer* **88**, 398–406.

- Hall, E. J. & Wu, C. S. (2003) *Int. J. Radiat. Oncol. Biol. Phys.* **56**, 83–88.
- Farkas, A., Schneider, D., Perrotti, M., Cummings, K. B. & Ward, W. S. (1998) *Urology* **52**, 444–448.
- Brady, L. W., Kramer, S., Levitt, S. H., Parker, R. G. & Powers, W. E. (2001) *Radiology* **219**, 1–5.

6. Gray, L. H. (1965) in *Cellular Radiation Biology; A Symposium Considering Radiation Effects in the Cell and Possible Implications for Cancer Therapy, a Collection of Papers* (Williams & Wilkins, Baltimore), pp. 8–25.
7. Mole, R. H. (1975) *Br. J. Radiol.* **48**, 157–169.
8. Hall, E. J. (2000) *Radiobiology for the Radiologist* (Lippincott, Williams & Wilkins, Philadelphia).
9. Nias, A. H. W. & Duncan, W. (1988) *Clinical Radiobiology* (Churchill Livingstone, Edinburgh, U.K.).
10. Shimizu, Y., Kato, H. & Schull, W. J. (1990) *Radiat. Res.* **121**, 120–141.
11. Zaider, M. (1991) *Health Phys.* **61**, 631–636.
12. Brenner, D. J. (1993) *Health Phys.* **65**, 358–366.
13. Radivoyevich, T. & Hole, D. G. (2000) *Radiat. Environ. Biophys.* **39**, 153–159.
14. Little, M. P. (2001) *Int. J. Radiat. Biol.* **77**, 431–464.
15. Bennett, J., Little, M. P. & Richardson, S. (2004) *Radiat. Environ. Biophys.* **43**, 233–245.
16. Travis, L. B., Hill, D. A., Dores, G. M., Gospodarowicz, M., van Leeuwen, F. E., Holowaty, E., Glimelius, B., Andersson, M., Wiklund, T., Lynch, C. F., *et al.* (2003) *J. Am. Med. Assoc.* **290**, 465–475.
17. van Leeuwen, F. E., Klokman, W. J., Stovall, M., Dahler, E. C., van't Veer, M. B., Noordijk, E. M., Crommelin, M. A., Aleman, B. M., Broeks, A., Gospodarowicz, M., *et al.* (2003) *J. Natl. Cancer Inst.* **95**, 971–980.
18. Gilbert, E. S., Stovall, M., Gospodarowicz, M., Van Leeuwen, F. E., Andersson, M., Glimelius, B., Joensuu, T., Lynch, C. F., Curtis, R. E., Holowaty, E., *et al.* (2003) *Radiat. Res.* **159**, 161–173.
19. Land, C. E., Tokunaga, M., Koyama, K., Soda, M., Preston, D. L., Nishimori, I. & Tokuoka, S. (2003) *Radiat. Res.* **160**, 707–717.
20. Thompson, D. E., Mabuchi, K., Ron, E., Soda, M., Tokunaga, M., Ochikubo, S., Sugimoto, S., Ikeda, T., Terasaki, M., Izumi, S., *et al.* (1994) *Radiat. Res.* **137**, S17–S67.
21. Land, C. E., Gilbert, E. & Smith, J. M. (2003) *Report of the NCI-CDC Working Group to Revise the 1985 NIH Radioepidemiological Tables* (National Institutes of Health, Bethesda), NIH Publication 03-5387.
22. Hopewell, J. W., Nyman, J. & Turesson, I. (2003) *Int. J. Radiat. Biol.* **79**, 513–524.
23. Kasper, M. & Fehrenbach, H. (2000) *Int. J. Radiat. Biol.* **76**, 493–501.
24. Brown, J. M. (1970) *Radiat. Res.* **43**, 627–653.
25. Judas, L., Bentzen, S. M., Hansen, P. V. & Overgaard, J. (1996) *Cell Prolif.* **29**, 73–87.
26. Dorr, W. & Kummermehr, J. (1990) *Radiother. Oncol.* **17**, 249–259.
27. Sacher, G. A. & Trucco, E. (1966) *Radiat. Res.* **29**, 236–256.
28. Yakovlev, A. & Polig, E. (1996) *Math. Biosci.* **132**, 1–33.
29. Holt, P. D. (1997) *Int. J. Radiat. Biol.* **71**, 203–213.
30. Wheldon, E. G., Lindsay, K. A. & Wheldon, T. E. (2000) *Int. J. Radiat. Biol.* **76**, 699–710.
31. Heidenreich, W. F., Jacob, P. & Paretzke, H. G. (1997) *Radiat. Environ. Biophys.* **36**, 45–58.
32. Little, M. P. (2001) *Lancet Oncol.* **2**, 212–220.
33. Lindsay, K. A., Wheldon, E. G., Deehan, C. & Wheldon, T. E. (2001) *Br. J. Radiol.* **74**, 529–536.
34. Bell, D. R. & Van Zant, G. (2004) *Oncogene* **23**, 7290–7296.
35. Dorr, W. (1998) *Strahlenther. Onkol.* **174** Suppl. 3, 4–7.
36. Clarke, R. B., Anderson, E., Howell, A. & Potten, C. S. (2003) *Cell Prolif.* **36** Suppl. 1, 45–58.
37. Reya, T., Morrison, S. J., Clarke, M. F. & Weissman, I. L. (2001) *Nature* **414**, 105–111.
38. Hall, E. J. & Brenner, D. J. (1991) *Int. J. Radiat. Oncol. Biol. Phys.* **21**, 1403–1414.
39. Brenner, D. J. & Hall, E. J. (1991) *Int. J. Radiat. Oncol. Biol. Phys.* **20**, 181–190.
40. van de Geijn, J. (1988) *Radiother. Oncol.* **12**, 57–78.
41. Chang, W. P. & Little, J. B. (1992) *Carcinogenesis* **13**, 923–928.
42. Held, K. D. (1997) *Apoptosis* **2**, 265–282.
43. Trott, K. R., Jamali, M., Manti, L. & Teibe, A. (1998) *Int. J. Radiat. Biol.* **74**, 787–791.
44. Walsh, L., Ruhm, W. & Kellerer, A. M. (2004) *Radiat. Environ. Biophys.* **43**, 225–231.
45. Jemal, A., Tiwari, R. C., Murray, T., Ghafoor, A., Samuels, A., Ward, E., Feuer, E. J. & Thun, M. J. (2004) *CA Cancer J. Clin.* **54**, 8–29.
46. Preston, D. L., Kusumi, S., Tomonaga, M., Izumi, S., Ron, E., Kuramoto, A., Kamada, N., Dohy, H., Matsuo, T., Matsui, T., *et al.* (1994) *Radiat. Res.* **137**, S68–S97.
47. Travis, L. B., Curtis, R. E., Storm, H., Hall, P., Holowaty, E., Van Leeuwen, F. E., Kohler, B. A., Pukkala, E., Lynch, C. F., Andersson, M., *et al.* (1997) *J. Natl. Cancer Inst.* **89**, 1429–1439.
48. Glatstein, E. (2002) *Semin. Radiat. Oncol.* **12**, 272–281.